

## Right-handed currents in $B \rightarrow K^* \ell^+ \ell^-$

---

**Rusa Mandal**<sup>\*†</sup>

*The Institute of Mathematical Sciences, Taramani, Chennai 600113, India  
and*

*Homi Bhabha National Institute Training School Complex, Anushakti Nagar, Mumbai 400085,  
India*

*E-mail:* [rusam@imsc.res.in](mailto:rusam@imsc.res.in)

The rare decay  $B \rightarrow K^* \ell^+ \ell^-$  is an important mode for indirect search of new physics (NP) due to the measurement of large number of observables in experiments. Using the most general parametric form of the amplitude in the standard model (SM), we probe the physics beyond standard model in a theoretically clean approach. The model independent framework has been implemented in the maximum  $q^2$  limit to highlight strong evidence of right-handed currents, which are absent in the SM. The conclusions derived are free from hadronic corrections. Our approach differs from other approaches that probe new physics at low  $q^2$  as it does not require estimates of hadronic parameters but relies instead on heavy quark symmetries that are reliable at the maximum  $q^2$  kinematic endpoint.

*9th International Workshop on the CKM Unitarity Triangle  
28 November - 3 December 2016  
Tata Institute for Fundamental Research (TIFR), Mumbai, India*

---

<sup>\*</sup>Speaker.

<sup>†</sup>in collaboration with Rahul Sinha, Thomas E. Browder, Abinash Kumar Nayak, Anirban Karan.

## 1. Introduction

The rare decay  $B \rightarrow K^* \ell^+ \ell^-$  involves a  $b \rightarrow s$  flavor changing loop induced transition and hence are very suppressed in the standard model (SM). The rich angular analysis of this mode leads us to measure plethora of observables at experiments and thus currently is of great interest to both theory as well as experimental groups. To probe new physics (NP) in this mode, one has to be certain about all possible contributions within the SM and hence requires for clean approaches i.e., those have reduced dependency on hadronic uncertainties. In this note, we briefly discuss the results obtained in our recent studies on this mode and refer the reader to Refs. [1, 2, 3] for detailed description.

## 2. Right handed current analysis

In this section first we briefly discuss the theoretical framework adopted to comprehensively consider almost all possible contributions within the SM for the decay  $B \rightarrow K^* \ell^+ \ell^-$  and then use the model independent framework to look for a possible new physics (NP) scenario i.e., right handed (RH) currents. We start with the observables as defined in Ref. [1] to be the well known longitudinal helicity fraction  $F_L$  and three observables  $F_\perp$ ,  $A_5$ ,  $A_{\text{FB}}$  which are related to the  $CP$  averaged observables  $S_3$ ,  $S_5$ ,  $A_{\text{FB}}^{\text{LHCb}}$  measured by LHCb [4] as follows:

$$F_\perp = \frac{1 - F_L + 2S_3}{2}, \quad A_5 = \frac{3}{4}S_5, \quad A_{\text{FB}} = -A_{\text{FB}}^{\text{LHCb}}. \quad (2.1)$$

The observables are functions of transversity amplitudes and in the massless lepton limit the decay is described by six transversity amplitudes which can be written in the most general form as [1],

$$\mathcal{A}_\lambda^{L,R} = (\tilde{C}_9^\lambda \mp C_{10}) \mathcal{F}_\lambda - \tilde{\mathcal{G}}_\lambda. \quad (2.2)$$

This parametric form of SM amplitude includes all short-distance and long-distance effects, factorizable and non-factorizable contributions and resonance contributions. In Eq. (2.2),  $C_9$  and  $C_{10}$  are Wilson coefficients with  $\tilde{C}_9^\lambda$  being the redefined ‘‘effective’’ Wilson coefficient defined [1] as

$$\tilde{C}_9^\lambda = C_9 + \Delta C_9^{(\text{fac})}(q^2) + \Delta C_9^{\lambda,(\text{non-fac})}(q^2), \quad (2.3)$$

where  $\Delta C_9^{(\text{fac})}(q^2)$ ,  $\Delta C_9^{\lambda,(\text{non-fac})}(q^2)$  correspond to factorizable and soft gluon non-factorizable contributions.  $\mathcal{F}_\lambda$  and  $\tilde{\mathcal{G}}_\lambda$  are the form factors for the decay mode. The RH current operators  $O'_9$  and  $O'_{10}$ , with respective couplings  $C'_9$  and  $C'_{10}$ , modify the amplitudes as follows

$$\mathcal{A}_\perp^{L,R} = ((\tilde{C}_9^\perp + C'_9) \mp (C_{10} + C'_{10})) \mathcal{F}_\perp - \tilde{\mathcal{G}}_\perp, \quad \mathcal{A}_{\parallel,0}^{L,R} = ((\tilde{C}_9^{\parallel,0} - C'_9) \mp (C_{10} - C'_{10})) \mathcal{F}_{\parallel,0} - \tilde{\mathcal{G}}_{\parallel,0} \quad (2.4)$$

With the introduction of notation:  $r_\lambda = \text{Re}(\tilde{\mathcal{G}}_\lambda)/\mathcal{F}_\lambda - \text{Re}(\tilde{C}_9^\lambda)$ ,  $\xi = C'_{10}/C_{10}$ , and  $\xi' = C'_9/C_{10}$ , we construct the following variables,

$$R_\perp = \left( \frac{r_\perp}{C_{10}} - \xi' \right) / (1 + \xi), \quad R_{\parallel,0} = \left( \frac{r_{\parallel,0}}{C_{10}} + \xi' \right) / (1 - \xi). \quad (2.5)$$

At low recoil energy of  $K^*$  meson, only three independent form factors describe the whole  $B \rightarrow K^* \ell^+ \ell^-$  decay and there exist a relation among the form factors at leading order in  $1/m_B$

expansion given by [5, 6],  $\tilde{\mathcal{G}}_{\parallel}/\mathcal{F}_{\parallel} = \tilde{\mathcal{G}}_{\perp}/\mathcal{F}_{\perp} = \tilde{\mathcal{G}}_0/\mathcal{F}_0 = -\kappa 2m_b m_B C_7/q^2$ , where  $\kappa \approx 1$ . Hence at the maximum point in  $q^2$  i.e., the kinematic endpoint  $q_{\max}^2$ , one defines  $r$  such that  $r_0 = r_{\parallel} = r_{\perp} \equiv r$ . Therefore Eq. (2.5) implies that in the presence of RH currents one should expect  $R_0 = R_{\parallel} \neq R_{\perp}$  at  $q^2 = q_{\max}^2$  without any approximation. Interestingly, this relation is unaltered by non-factorizable and resonance contributions [7] at this kinematic endpoint. To test the relation among  $R_{\lambda}$ 's in light of LHCb data, first defining  $\delta \equiv q_{\max}^2 - q^2$ , we expand the observables  $F_L, F_{\perp}, A_{\text{FB}}$  and  $A_5$  around  $q_{\max}^2$  as follows:

$$\begin{aligned} F_L &= \frac{1}{3} + F_L^{(1)}\delta + F_L^{(2)}\delta^2 + F_L^{(3)}\delta^3, & F_{\perp} &= F_{\perp}^{(1)}\delta + F_{\perp}^{(2)}\delta^2 + F_{\perp}^{(3)}\delta^3, \\ A_{\text{FB}} &= A_{\text{FB}}^{(1)}\delta^{1/2} + A_{\text{FB}}^{(2)}\delta^{3/2} + A_{\text{FB}}^{(3)}\delta^{5/2}, & A_5 &= A_5^{(1)}\delta^{1/2} + A_5^{(2)}\delta^{3/2} + A_5^{(3)}\delta^{5/2}. \end{aligned} \quad (2.6)$$

The zeroth order coefficients of the observable expansions are assumed from the constraints arising from Lorentz invariance and decay kinematics derived in Ref. [7], whereas all the higher order coefficients are extracted by fitting the polynomials with 14 bin LHCb data as shown in Fig. 1.

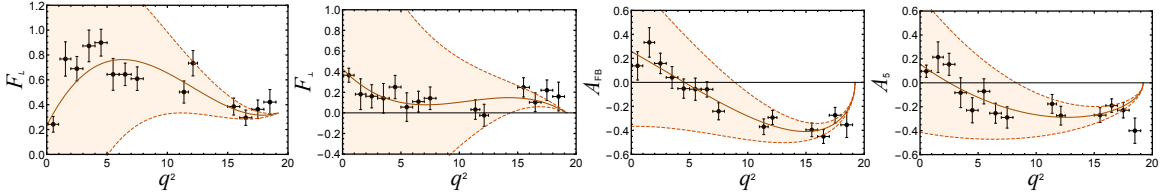


**Figure 1:** An analytic fit to 14-bin LHCb data using Taylor expansion at  $q_{\max}^2$  for the observables  $F_L, F_{\perp}, A_{\text{FB}}$  and  $A_5$  are shown as the brown curves. The  $\pm 1\sigma$  error bands are indicated by the light brown shaded regions, derived including correlation among all observables. The points with the black error bars are LHCb 14-bin measurements [4].

The limiting analytic expressions for  $R_{\lambda}$  at  $q^2 = q_{\max}^2$  are

$$R_{\perp}(q_{\max}^2) = \frac{\omega_2 - \omega_1}{\omega_2 \sqrt{\omega_1 - 1}}, \quad R_{\parallel}(q_{\max}^2) = \frac{\sqrt{\omega_1 - 1}}{\omega_2 - 1} = R_0(q_{\max}^2) \quad (2.7)$$

$$\text{where } \omega_1 = 3F_{\perp}^{(1)2}/2A_{\text{FB}}^{(1)2} \text{ and } \omega_2 = 4 \left( 2A_5^{(2)} - A_{\text{FB}}^{(2)} \right) / 3A_{\text{FB}}^{(1)} \left( 3F_L^{(1)} + F_{\perp}^{(1)} \right). \quad (2.8)$$

It can be seen that  $\omega_1, \omega_2$  contain coefficients which are extracted completely from data and their estimates using LHCb measurements are:  $\omega_1 = 1.10 \pm 0.30$  ( $1.03 \pm 0.34$ ) and  $\omega_2 = -4.19 \pm 10.48$  ( $-4.04 \pm 10.12$ ), where the first values are determined using  $A_{\text{FB}}^{(1)}$  and the values in the round brackets use  $2A_5^{(1)}$ . The variables  $R_{\lambda}$ 's can be estimated using data only and the allowed region is shown in gray bands in Fig. 2 left panel. A significant deviation is seen from a slope of  $45^\circ$  line (red line) which denotes  $R_{\perp} = R_{\parallel} = R_0$  and thus hints toward the presence of RH currents without using any estimate of hadronic contributions. To quantify the RH couplings, we use Eq. (2.5) and the results are shown in the last two panels of Fig. 2. The middle panel uses the SM estimate of parameter  $r/C_{10}$  [6] and the SM prediction for  $C'_{10}/C_{10}$  and  $C'_9/C_{10}$  (the origin) is at more than  $5\sigma$  confidence level. We have performed another analysis where the input  $r/C_{10}$  is considered as nuisance parameter and the result is shown in the right most panel of Fig. 2. It can be seen that the uncertainties in fitted parameters  $C'_{10}/C_{10}$  and  $C'_9/C_{10}$  have increased due to the variation of  $r/C_{10}$  and the SM prediction still remains on a  $3\sigma$  level contour providing evidence of RH currents.

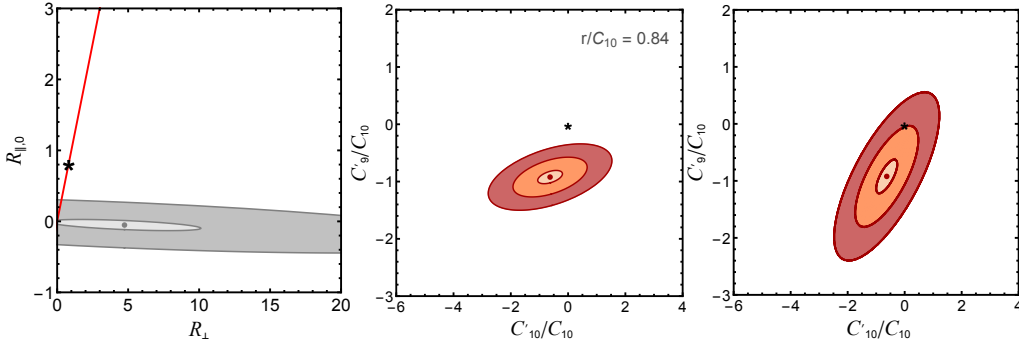


**Figure 2:** (left panel) Allowed regions in  $R_{\perp} - R_{\parallel,0}$  plane are shown in light and dark gray bands at  $1\sigma$  and  $5\sigma$  confidence level, respectively. The red straight line corresponds to the case  $R_{\perp} = R_{\parallel,0}$  i.e. the absence of RH couplings. (middle panel) In  $C'_{10}/C_{10} - C'_9/C_{10}$  plane, the yellow, orange and red regions correspond to  $1\sigma$ ,  $3\sigma$  and  $5\sigma$  significance level, respectively, where SM input for  $r/C_{10}$  [6] is used. The best fit values of  $C'_{10}/C_{10}$  and  $C'_9/C_{10}$ , with  $\pm 1\sigma$  errors are  $-0.63 \pm 0.43$  and  $-0.92 \pm 0.10$ , respectively. (right panel) Same color code as the middle panel figure. The input  $r/C_{10}$  is varied as a nuisance parameter and hence the obtained uncertainties in  $C'_{10}/C_{10}$  and  $C'_9/C_{10}$  are increased. The SM predictions for all the three plots are indicated by the stars. Strong evidence of RH current is pronounced from the plots.

### 3. Some sanity checks

#### 3.1 Resonance effects

Resonances can alter the results that are obtained using a polynomial fit to the observables in Eq. (2.6), where it is assumed that resonances are absent. To study the systematics due to resonances, we assume observables calculated using theoretical estimates of form factors (LCSR [8] for  $q^2 \leq 15\text{GeV}^2$  and Lattice QCD [9] for  $q^2 \geq 15\text{GeV}^2$  region) and Wilson coefficients. Following the parametrization from Ref. [10], we include the  $J/\psi(1S)$ ,  $\psi(2S)$ ,  $\psi(3770)$ ,  $\psi(4040)$ ,  $\psi(4160)$  and  $\psi(4415)$  resonances in our study. The procedure uses the function  $g(m_c, q^2)$ , in Wilson coefficient  $C_9^{\text{eff}}$ , which includes the cross-section ratio  $R_{\text{had}}^{c\bar{c}}(q^2) = R_{\text{cont}}^{c\bar{c}}(q^2) + R_{\text{res}}^{c\bar{c}}(q^2)$ , where the resonance effects are incorporated as

$$R_{\text{res}}^{c\bar{c}}(q^2) = N_r \sum_{V=J/\psi, \psi'..} \frac{9q^2 \text{Br}(V \rightarrow \ell^+ \ell^-) \Gamma_{\text{tot}}^V \Gamma_{\text{had}}^V}{\alpha (q^2 - m_V^2)^2 + m_V^2 \Gamma_{\text{tot}}^V} e^{i\delta_V}. \quad (3.1)$$

Here  $\Gamma_{\text{tot}}^V$  is the total width of the vector meson ‘V’,  $\delta_V$  is an arbitrary relative strong phase associated with each of the resonances and  $N_r$  is a normalization factor that fixes the size of the resonance contributions compared to the non-resonant background. A random simulation has been done by varying each resonance phases  $\delta_V$  and a sample of plots for different observables are given in link [11] as movies. It can be seen from the plots that when resonances are included,  $A_{\text{FB}}$  and  $A_5$  always decrease in magnitude for the  $15\text{GeV}^2 \leq q^2 \leq 19\text{GeV}^2$  region. Hence if the effect of resonances could somehow be removed from the data, the values of  $A_{\text{FB}}$  and  $A_5$  would be larger in magnitude which in turn will decrease the value of observable  $\omega_1$  compared to the values obtained from fits to experimental data in which resonances are automatically present. As the current obtained values of  $\omega_1$  from data are already close to unity, any further reduction will force  $\omega_1$  into the un-physical domain and increase the significance of deviation from the SM.

### 3.2 Polynomial fit convergence

In this section, we study the systematics of the fits to coefficients  $A_{\text{FB}}^{(1)}$ ,  $A_{\text{FB}}^{(2)}$ ,  $F_L^{(1)}$ ,  $A_5^{(1)}$ ,  $A_5^{(2)}$  and  $F_{\perp}^{(1)}$ , which appear in the expressions of  $\omega_1$  and  $\omega_2$  given in Eq. (2.8). By varying the order of the polynomial fitted, from 2 to 4, and also the number of bins from the last 4 to 14 bins, each extracted coefficients are shown in Fig. 3. We find that all the fitted coefficients show a good degree of convergence even when larger number of bins are added. The values obtained for the coefficients are consistent within  $\pm 1\sigma$  regions apart from some small mismatches in  $F_{\perp}^{(1)}$  and  $A_5^{(1)}$ . We choose as a benchmark the third order polynomial fit to all 14 bins and to validate this choice, we also perform an identical fit for observables generated using form factor values [8, 9] and the results are shown in Fig. 4. The fits to SM observables are satisfactory for the entire  $q^2$  region.

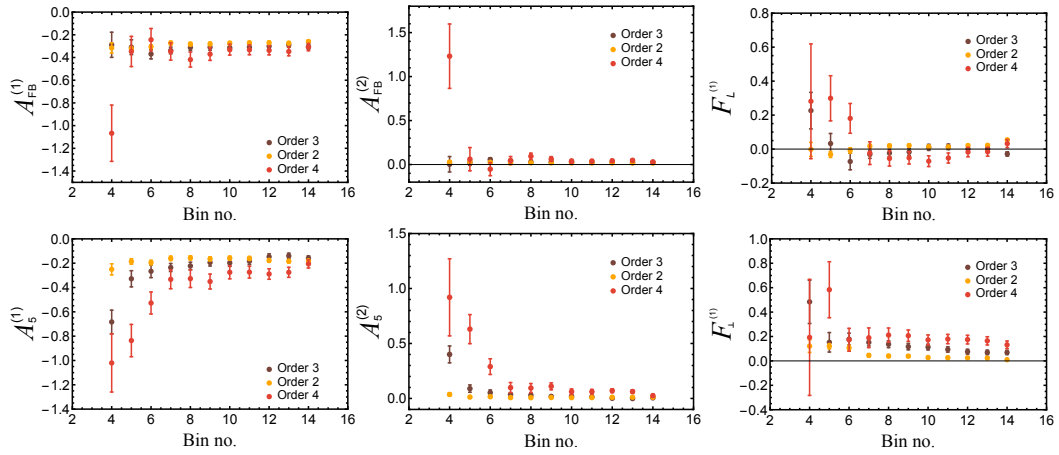


**Figure 3:** Systematic study of the coefficients of observables with the variation of polynomial order and the number of bins used for the fit. The color code for the different orders of the fitted polynomial is depicted in the panel. The  $x$ -axis denotes the number of bins used for the fit from last 4 to 14 bins. Coefficient values show good convergence within the  $\pm 1\sigma$  error bars except for few bins in the  $F_{\perp}^{(1)}$  and  $A_5^{(1)}$  distributions. The 4-bin order 4 polynomial fit shows disagreement which is expected.

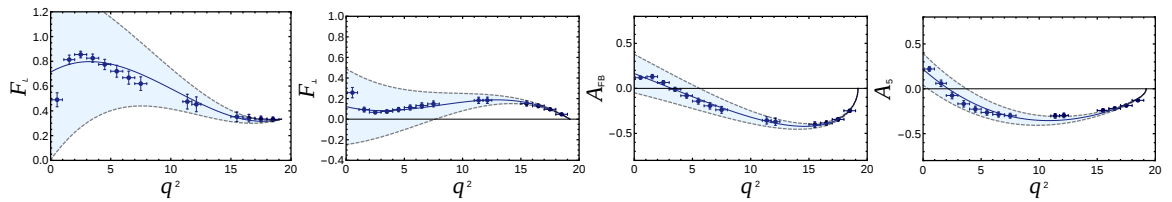


**Figure 4:** Fits with third order polynomials to the theoretical SM observables, generated using LCSR form factors for  $q^2 \leq 15\text{GeV}^2$  [8] and Lattice QCD form factors for  $q^2 \geq 15\text{GeV}^2$  [9]. The blue error bars are bin integrated SM estimates and the solid blue curve with the shaded region represents the best fit polynomial with  $\pm 1\sigma$  errors. The fits nicely explain the SM observables including the zero-crossing of asymmetries  $A_{\text{FB}}$  and  $A_5$ .

#### 4. Summary

- A formalism has been developed to incorporate almost all possible effects within the SM. The approach we have adopted in our work differs from the other approaches [12] in literature as we have no or minimal dependency on hadronic uncertainties.
- A strong evidence of RH currents is found where the conclusions are derived at endpoint limit.
- The detailed study of resonance effects strengthen the conclusion derived here.
- A systematic study, by varying the polynomial order (Eq. (2.6)) and the number of bins used to fit the polynomials, shows a very good convergence for fit coefficients.
- The finite width effect of  $K^*$  meson has also been considered where the position of the kinematic endpoint  $q_{\max}^2$  is varied over a range considering width of  $K^* \sim 50\text{MeV}$ . Using a weighted average over the Breit-Wigner shape for  $K^*$  meson, the  $\omega_1$  and  $\omega_2$  values are found well within the  $\pm 1\sigma$  uncertainties of the results obtained without the width effect.
- We conclude that there is a need for more data from experiments to confirm the presence of the NP scenario presented here.

#### References

- [1] R. Mandal, R. Sinha and D. Das, Phys. Rev. D **90**, no. 9, 096006 (2014).
- [2] R. Mandal and R. Sinha, Phys. Rev. D **95**, no. 1, 014026 (2017).
- [3] A. Karan, R. Mandal, A. K. Nayak, R. Sinha and T. E. Browder, arXiv:1603.04355 [hep-ph].
- [4] R. Aaij *et al.* [LHCb Collaboration], JHEP **1602**, 104 (2016).
- [5] B. Grinstein, D. Prijol, Phys. Rev. D **70** 114005 (2004),
- [6] C. Bobeth, G. Hiller and D. van Dyk, JHEP **1007**, 098 (2010).
- [7] G. Hiller, Roman Zwicky, JHEP **1403**, 042 (2014).
- [8] A. Bharucha, D. M. Straub and R. Zwicky, JHEP **1608**, 098 (2016);
- [9] R. R. Horgan, Z. Liu, S. Meinel and M. Wingate, Phys. Rev. Lett. **112**, 212003 (2014);
- [10] F. Kruger and L. M. Sehgal, Phys. Lett. B **380**, 199 (1996) [hep-ph/9603237].
- [11] <http://www.imsc.res.in/~abinashkn/arXiv>
- [12] W. Altmannshofer and D. M. Straub, Eur. Phys. J. C **75**, no. 8, 382 (2015),  
M. Ciuchini *et al.* JHEP **1606**, 116 (2016),  
S. Jäger and J. Martin Camalich, Phys. Rev. D **93** (2016) 1, 014028,  
S. Descotes-Genon, L. Hofer, J. Matias and J. Virto, JHEP **1606**, 092 (2016).